Numerical Modeling of Boiling in a Heated Tube

Alok Majumdar[1], Carmen Ursachi[2], Andre LeClair[1], and Jason Hartwig[3]

Abstract

This paper presents numerical models of boiling in a heated tube using the Generalized Fluid System Simulation Program (GFSSP), a finite-volume-based general-purpose flow network code developed at NASA/Marshall Space Flight Center. The heated tube is discretized into a one-dimensional array of nodes and branches to represent the flow of liquid and vapor in a tube with a prescribed pressure differential. The solid wall is also discretized into solid nodes and conductors to allow for heat transfer between the wall and the fluid. The conservation equations of mass, momentum, and energy of the fluid are solved simultaneously with the energy conservation equation for the solid wall. Two experimental configurations of fluid flowing in a vertical tube have been simulated, one with water and the other with liquid hydrogen. This paper compares experimental data with numerical predictions based on four different published correlations for boiling heat transfer coefficients. Three of these correlations are applicable to the saturated vertical flow conditions of the experiments. One of them is applicable to film boiling and has been used for the liquid hydrogen experiment, which was in film boiling regime. For the case of boiling water, the predictions of wall temperatures using the boiling heat transfer correlations agreed well with the experimental results. However, in the case of boiling hydrogen larger discrepancies were observed between the experimental data and numerical predictions.

[1] NASA/Marshall Space Flight Center
[2]Graduate Student at Massachusetts Institute of Technology, Summer Intern at NASA/Marshall Space Flight Center
[3]NASA/Glenn Research Center

1. Introduction

The combination of flowing cryogenic fluid and large temperature differences between the surroundings and fluids implies that there will be complex flow boiling, heat transfer, and two-phase flow patterns. Accurate prediction tools of cryogenic two-phase flow boiling and heat transfer are required to design, analyze, and size efficient cryogenic transfer systems both on the ground and in microgravity. Penalties for poor models include increased safety factors, higher margins, and overall increases in cost. The importance of flow boiling to a wide range of applications has driven a push to develop so-called universal correlations [1-4] that would aid in the design and analysis of all fluid transfer systems. While these correlations cover a broad range of conditions for predicting heat flux and pressure drop, they do not cover cryogenic fluids [5, 6].

There are two types of flow boiling encountered in cryogenic propellant transfer, quenching (or chill down) and heating. In the quenching configuration, the initial wall temperature is much higher than the initial bulk fluid temperature, and the fluid is used to

cool the hot tube. The quench test is a transient process where the heat flux and wall temperature are both changing with time. In contrast, the heating configuration is a steady state case where the initial temperature of the fluid and wall are equal and then heat is input into the liquid. In the former case, the fluid traverses the boiling curve from right to left (film to transition to nucleate boiling to single phase liquid convection) while in the latter case, the fluid traverses the boiling curve from left to right (single phase liquid convection to nucleate boiling and so on).

Recently, correlations were developed for cryogenic flow boiling, but in the quenching configuration [7]. The correlations were tested in GFSSP and SINDA FLUINT and results showed significant improvement in liquid nitrogen chilldown, and modest improvement in liquid hydrogen chilldown [8, 9]. Meanwhile for the heating configuration, as in the case of the quenching configuration, comparison of heated tube cryogenic data with available correlations show that existing correlations do not accurately predict cryogenic heated tube data, but the disparity between heated tube data and models is not nearly as high as in the quenching configuration [6]. Therefore, there should be less error in lumped node modeling of heated tube cases over quenching cases.

Accurate lumped node modeling of heated tube or steady state cryogenic flow is required for many space cryogenic transfer system applications. For example, after initial chilldown of the transfer line that connects a refueling element or depot storage tank to a customer receiver tank, modeling of the steady state transfer is required to determine the amount of subcooled margin needed in the tank upstream. Another example is the transfer of liquid hydrogen from the nuclear thermal propulsion storage tank to the reactor downstream (after the initial chilldown transients); subcooled liquid hydrogen flows from the tank to the reactor inlet and the hydrogen must be a gas when it reaches the reactor. Modeling of the steady state transfer is thus required to model vaporization of the fluid, design the entire feed system, to know where to place the pumps, etc.

Numerical modeling of the boiling in a heated tube is challenging due to the two-phase nature of flow with phase changes. Two phase flows can be modelled assuming the flow of liquid and vapor is homogeneous and move with the same speed. With the homogeneous assumptions [10,20], it is no longer necessary to solve for the separate conservation equations for mass, momentum and energy for the liquid and vapor phases to develop a numerical model for two phase flows. A single set of conservation equations for mass, momentum and energy can be solved using the properties of the liquid-vapor mixture. The accuracy of the numerical predictions, however, largely depend on the accuracy of boiling heat transfer correlations.

In the past there were several investigations [8,11,12] where chill down of cryogenic transfer lines has been numerically simulated by analyzing one-dimensional two phase flow using a homogeneous model. In those investigations, a general purpose flow network code, GFSSP (Generalized Fluid System Simulation Program) [13] has been used for numerical simulation. GFSSP is a finite volume based network flow analysis code developed at NASA/Marshall Space Flight Center. A reasonable comparison of numerical

predictions with analytical solution [11] and experimental data for long [12] and short [8] transfer lines has been demonstrated.

In this paper GFSSP has been used to develop a numerical model of flow in a heated tube. Two experimental situations are considered to compare the numerical predictions with the experimental data. In 1960, Sani [14] conducted an experiment investigating the boiling of water flowing up a vertical tube. Hendricks et al. [15] carried out an experiment studying the boiling heat transfer of hydrogen flowing down a vertical tube in 1961. The computational models of both experiments were developed and run using the correlations of Chen [16], Kandilkar [17], and Kim and Mudawar [18]. For the liquid hydrogen experiment, the film boiling correlation of Miropolski [19] was used. In order to calculate pressure drop in two-phase flow through pipe, Friedel's [20] correlation was used.

2. Experimental Configurations

Sani [14] conducted an experiment investigating the boiling of water flowing down a vertical tube. Pressure and temperature measurements were taken along the 68 in long heated 304 stainless steel tube. The tube had an inner diameter of 0.7194 in and a wall thickness of 0.015 in. The mass flow rate was measured via weight data and a Fisher-Porter rotameter. The rotameter was located upstream of the test section whereas the weight measurement was conducted downstream of the test section. Between these two methods the flow rates agreed within 1% of each other. Throughout the course of the experiment the mass flow rate, heat flux, inlet quality, and inlet pressure were varied.

Hendricks et al. [15] experimentally studied the boiling heat transfer of hydrogen flowing up a vertical tube. During their experiment, the mass flow rate of hydrogen, inlet pressure, and heat flux were varied between runs. The test section was made from a 12 in Inconel tube with an inner diameter of 0.313 in and a wall thickness equal to 0.031 in. Outer wall temperature and fluid pressure data were gathered along the length of the test section. The mass flow rate was measured upstream and downstream of the test section using a venturi tube and orifice, respectively.

3. Computational Models

Figure 1 shows the model used to simulate Sani's experiment in GFSSP. The nodes are evenly spaced along the tube length. Each fluid node is connected to a solid node through a solid to fluid conductor. The tube wall thickness has been represented by one solid node in the radial direction along the tube length. The input characteristics for each solid node are its mass, material, and heat source. Stainless steel 304's thermal conductivity is prebuilt into GFSSP. Each solid node's heat source calculated from the change in enthalpy across the first and last location for which data is given divided by the number of solid nodes. This heat source value was applied to each of the solid nodes. The model also accounted for heat conduction along the axial direction.

To determine the heat transfer coefficient, the heat transfer coefficient correlations of Chen [16], Kandlikar [17], and Kim and Mudawar [18] were coded into separate Fortran user subroutines. The outputs were fed back into GFSSP so that GFSSP's calculations were done using these correlations' heat transfer coefficients. The film boiling correlation of Miropolski [19] is available in GFSSP's library.

The fluid nodes were connected using pipes with the appropriate dimensions from Sani's experiment. To model water flowing down the pipe, the pipe's angle with the gravity vector was set to zero in the simulation. No information was provided in either experiment about the roughness of the pipes used in the test section, so all pipes were assumed to be smooth. A user subroutine calculated the pipe resistance using the Friedel [12] correlation for two-phase flow.

The remaining inputs to the GFSSP models were the boundary conditions. Pressures were set at both boundary nodes. Since GFSSP uses an upwind scheme, the temperatures at the downstream boundary nodes had no effect on the model. As it was observed that setting the experimental inlet and outlet pressures to match the test data led to mass flow rates that did not match the test measurements, priority was given to matching the experimental inlet pressure and mass flow rate. Therefore, the outlet pressure was adjusted until the desired flow rates were met. Finally, the inlet quality was set in accordance with the experimental runs.

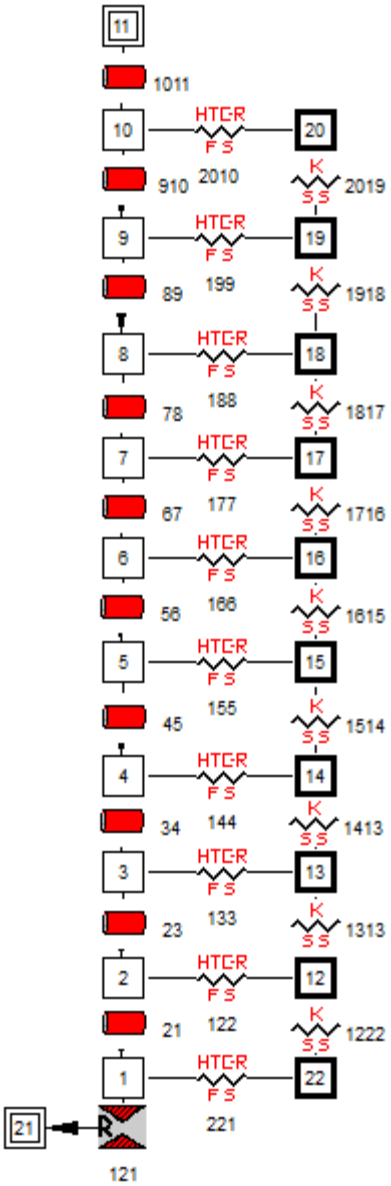

Figure 1. Single solid node model to represent wall constructed in GFSSP.

Two cases were selected from Sani's experiment: Run 5 and 32. The input conditions for these two cases are given in Table 1.

Table 1. Input Conditions for Two cases of Sani's Experiment

Run No.	Flowrate (lb/sec)	Inlet Pressure (psia)	Inlet Quality (%)	Heat Flux (Btu/hr-ft^2)
5	0.4641	18.73	1.57	10212
32	0.595	27.09	2.76	22776

Both cases were run with all three nucleate boiling heat transfer coefficient correlations. To verify the effect of discretization in the radial direction, solid wall was discretized into four nodes and results were compared with single wall node model. The difference between the predicted wall temperatures of two models was insignificant. Therefore, all computations were performed with single node representing the wall as shown in Figure 3.

The model created for Hendricks et al.'s experiment was very similar to Sani's. Unless explicitly noted, all model components were the same between these two experiments. After setting the appropriate dimensions and material/fluid properties, the inlet and outlet pressure and quality were set. Hendricks et al. provide data at 0.055" and 12" from the inlet of the 12" long test section. In this experiment, the flow was going in the opposite direction of gravity, so the pipe angle with respect to the gravity vector was set to 180°. This model was run with Kandlikar's and Kim and Mudawar's heat transfer coefficient correlations. It was found that Chen's correlation did not work for this model due to the large temperature differences between the fluid and wall temperatures for the boiling of hydrogen. But because of these high wall temperatures, the Hendricks case was also run with the Miropolski film boiling correlation. Two cases were selected from Hendricks et al.'s experiment Run 18-2 and 20-5. The input conditions for these two cases are given in Table 2.

Table 2. Input Conditions for Two cases of Hendricks et al's Experiment

Run No.	Flowrate (lb/sec)	Inlet Pressure (psia)	Inlet Quality (%)	Heat Flux (Btu/hr-ft^2)
18-2	0.177	45	0.4	77937
20-5	0.178	66.4	0	221519

4. Boiling Heat Transfer Correlations

4.1 Chen's Correlation

Chen [16] developed a boiling heat transfer correlation for use with water and organic fluids. The correlation was fit to saturated state data in the vertical flow direction. Chen's correlation is based on the principle of adding the macro-convective and micro-convective boiling components to calculate the two-phase heat transfer coefficient. The macro-convective portion is calculated using the fluid's properties at liquid conditions. The macro-convective component is the main heat transfer contributor for mostly liquid and low flow rate cases. It is described by an equation derived from the Dittus-Boelter equation:

$$h_{macro} = 0.023\, Re_l^{0.8}\, Pr_l^{0.4} \frac{F\, k_l}{D} \tag{1}$$

$$Re_l = \frac{G(1-x)D}{\mu_l} \tag{2}$$

$$Pr_l = \mu_l \frac{c_{p_l}}{k_l} \tag{3}$$

The Reynolds number factor, F can be determined graphically, or via the following graphical correlation by Collier [21]:

$$F = \begin{cases} 1 & \text{for} \dfrac{1}{X_{tt}} < 0.1 \\ 2.35\left(0.213 + \dfrac{1}{X_{tt}}\right)^{0.736} & \text{for} \dfrac{1}{X_{tt}} > 0.1 \end{cases} \tag{4}$$

X_{tt} is the Martinelli parameter.

$$X_{tt} = \left(\frac{\rho_v}{\rho_l}\right)^{0.5} \left(\frac{\mu_l}{\mu_v}\right)^{0.1} \left(\frac{1-x}{x}\right)^{0.9} \tag{5}$$

The micro-convective boiling component drives heat transfer in high vapor and high flow rate situations. The micro-convective heat transfer coefficient is derived from the assumption that the Rayleigh equation for bubble growth rate determines the Reynolds number. The resulting equation is as follows:

$$h_{micro} = 0.00122\, (\Delta T)^{0.24}\, (\Delta P)^{0.75}\, S \frac{k_l^{0.79}\, c_{p_l}^{0.45}\, \rho_l^{0.49}\, g_c^{0.25}}{\sigma^{0.5} \mu_l^{0.29}\, h_{fg}^{0.24}\, \rho_v^{0.24}} \tag{6}$$

where

$$\Delta T = T_w - T_{sat} \tag{7}$$

$$\Delta P = P_{sat}(T_w) - P \tag{8}$$

The suppression factor, S, can be found from the following curve fit equation by Collier [21].

$$S = [1 + (2.56 \times 10^{-6})(Re_l F^{1.25})^{1.17}]^{-1} \tag{9}$$

Finally, the two-phase heat transfer coefficient can be determined by adding the microconvective and macroconvective heat transfer coefficients.

$$h_{tp} = h_{macro} + h_{micro} \tag{10}$$

4.2 Kandlikar's Correlation

Kandlikar [17] developed a boiling heat transfer coefficient correlation that was intended to be general. It is applicable for both horizontal and vertical saturated tube flow. Kandlikar bases his correlation off a fluid database containing experimental data for water, refrigerants, and cryogens.

To determine the two-phase heat transfer coefficient using Kandlikar's correlation, the following is evaluated using the values provided in Table 2 for the constants:

$$h_{tp_{conv,nucl}} = h_l\left(C_1 Co^{C_2}(25Fr_l)^{C_5} + C_3 Bo^{C_4} F_{fl}\right) \tag{11}$$

where

$$h_l = 0.023 Re_l^{0.8} Pr_l^{0.4}\left(\frac{k_l}{D}\right) \tag{12}$$

Table 3. Values for constants used in Kandlikar's correlation

	Convective	Nucleate	
C_1	1.136	0.6683	
C_2	-0.9	-0.2	
C_3	667.2	1058.0	
C_4	0.7	0.7	
C_5	0.3	0.3	0 for vertical tubes, horizontal tube w/ $Fr_l > 0.04$

The Reynolds number and Prandtl number are evaluated at liquid-only conditions, as previously described in Eqs. (2) and (3). The convection number and boiling number are found via the following:

$$Co = \left(\frac{1-x}{x}\right)^{0.8} \left(\frac{\rho_v}{\rho_l}\right)^{0.5} \tag{13}$$

$$Bo = \frac{q}{Gh_{fg}} \tag{14}$$

The Froude number is defined as:

$$Fr_l = \frac{G^2}{\rho_l^2 gD} \tag{15}$$

It is only used in Eq. (13) when $Fr_l \leq 0.04$.

The heat transfer coefficient is calculated two separate times, once using the Table 3 constants corresponding to the convective component, and once using the values corresponding to the nucleate portion. The final two-phase heat transfer coefficient is equal to the maximum of the two-phase coefficients evaluated at solely convective or nucleate boiling conditions.

$$h_{tp} = \max\left(h_{tp_{conv}}, h_{tp_{nucl}}\right) \tag{16}$$

4.3 Kim and Mudawar's Correlation

Another correlation used in this study is the Kim and Mudawar [18] correlation for boiling heat transfer coefficients. The correlation was designed for use with flows in mini/micro channels. The fluids in this database are FC72, refrigerants, carbon dioxide, and water. The fluids have a reduced pressure between $0.005 < P_R < 0.69$. No information is given about the range of heat fluxes contained within the fluid database. The two-phase heat transfer coefficient is found via the following:

$$h_{tp} = \left(h_{tp_{nucl}}^2 + h_{tp_{conv}}^2\right)^{0.5} \tag{17}$$

The nucleate boiling portion is calculated as follows:

$$h_{tp_{nucl}} = \left[2345\left(Bo\frac{P_H}{P_F}\right)^{0.7} P_R^{0.38}(1-x)^{-0.51}\right]\left(0.023Re_l^{0.8}Pr_l^{0.4}\frac{k_l}{D_h}\right) \tag{18}$$

where

$$Bo = q_H / G h_{fg} \tag{19}$$

$$P_R = P / P_{crit} \tag{20}$$

P_H and P_F are the heated channel perimeter and wetted channel perimeter, respectively. For a circular tube, P_H and P_F are simply equal to the tube's perimeter. The convective boiling component is:

$$h_{tp_{conv}} = \left[5.2\left(Bo\frac{P_H}{P_F}\right)^{0.08} We_l^{-0.54} + 3.5\left(\frac{1}{X_{tt}}\right)^{0.94}\left(\frac{\rho_v}{\rho_l}\right)^{0.25}\right]\left(0.023 Re_l^{0.8} Pr_l^{0.4}\frac{k_l}{D_h}\right) \tag{21}$$

The liquid Reynolds number, liquid Prandtl number, and Martinelli parameter are calculated via Eqs. (2), (3), and (6), respectively. The Weber number, We_l, was introduced to take into consideration the effects of surface tension interacting with inertia.

$$We_l = \frac{G^2 D_h}{\rho_l \sigma} \tag{22}$$

4.4 Miropolski Correlation

The last correlation used in this study is the correlation of Miropolski [19], based on film boiling of water. A modified version of the Miropolski correlation is a standard option in GFSSP [13]. The film boiling heat transfer coefficient is found via the following:

$$h = 0.023\frac{k_v}{D} Re_{mix}^{0.8} Pr_v^{0.4} Y \tag{23}$$

where

$$Re_{mix} = \left(\frac{\rho u D}{\mu_v}\right)\left[x + \frac{\rho_v}{\rho_l}(1-x)\right] \tag{24}$$

$$Pr_v = \frac{C_{pv}\mu_v}{k_v} \tag{25}$$

$$Y = 1 - 0.1\left(\frac{\rho_l}{\rho_v}\right)^{0.4}(1-x)^{0.4} \tag{26}$$

The modified Miropolski correlation has been used previously to model the chilldown of transfer lines by liquid nitrogen and liquid hydrogen [8,11,12].

5. Results & Discussion

5.1 Sani's Experiment Model

The first run selected from Sani's experiment was Run 5 described in Table 1. To match the inlet pressure and mass flow rate, the outlet pressure had to be reduced by 1.33%. The pressure and fluid temperature throughout the test section are shown in Fig. 2 and 3, respectively. These computations were made using Sani's measured heat transfer coefficients and Friedel's [20] correlation for pressure drop. The predicted quality is compared with measured data in Figure 4.

Figure 5 shows the comparison of predicted heat transfer coefficient with the measured data. The correlations of Chen, Kandilkar, Kim and Mudawar were used in this analysis. Chen's correlation is closest to the measured value. Kim and Mudawar's correlation under predicts heat transfer coefficient. The predicted wall temperatures are shown in Figure 6 and compared with the measured wall temperatures. While Chen and Kandilkar's correlations match well with the measured data, Kim and Mudawar over predicts wall temperatures which is a consequence of under predicting heat transfer coefficient. Perhaps, Kim and Mudawar's correlation is more appropriate for mini or micro channels.

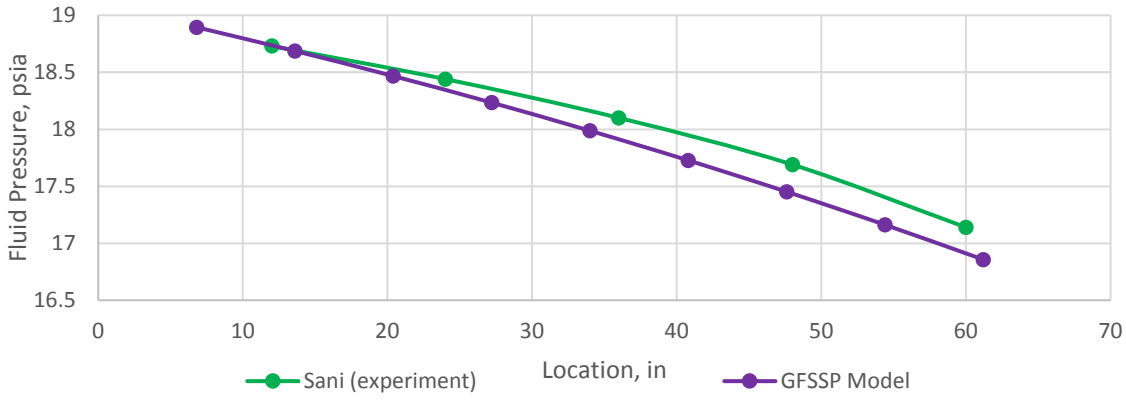

Figure 2. Comparison of Sani's experimentally measured pressures and GFSSP model for Run 5.

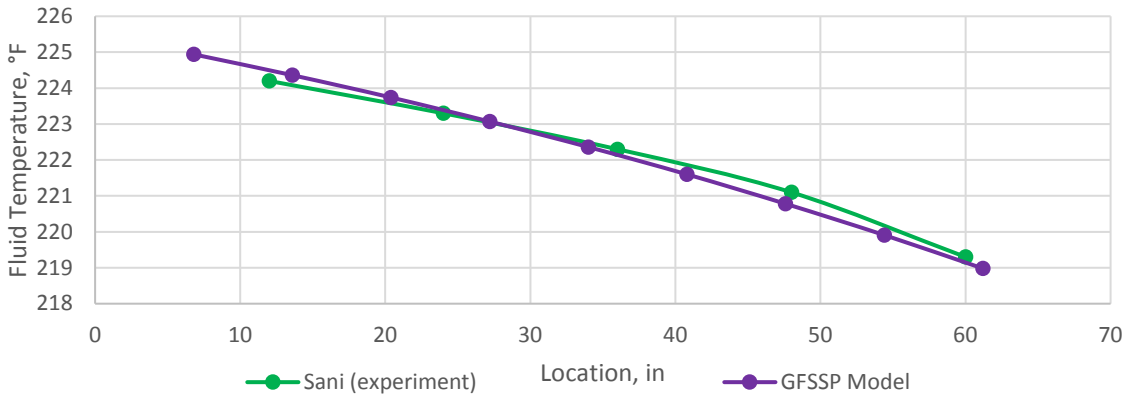

Figure 3. Comparison of Fluid Temperatures between Sani's experiment and GFSSP model for Run 5.

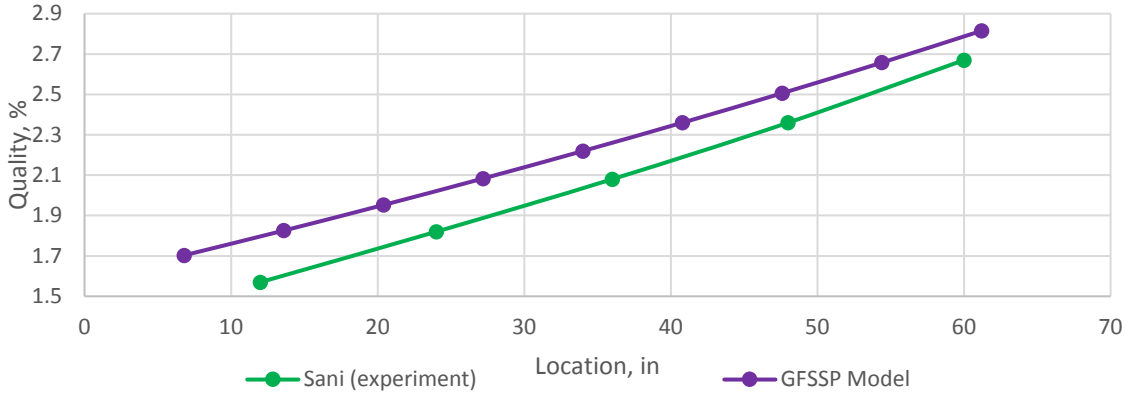

Figure 4. Comparison of Sani's reported qualities and GFSSP's values for Run 5.

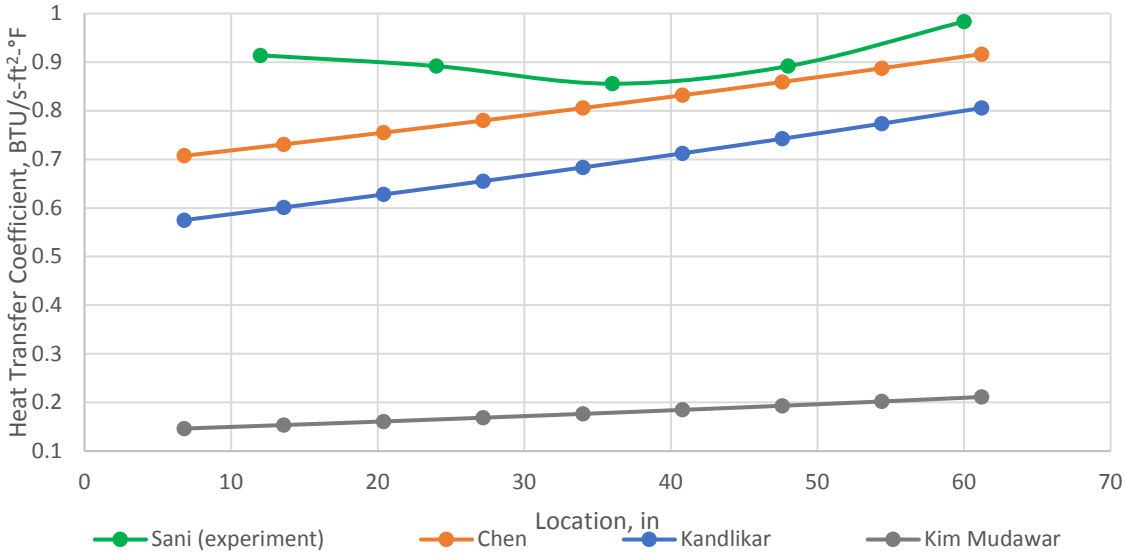

Figure 5. Predicted heat transfer coefficients from each correlation versus the experimental value for Sani's Run 5.

The next run discussed in this paper is Sani's Run 32 which has a higher mass flow rate, higher heat flux and operated at a higher pressure than previously discussed Run 5 (Table 1). With this higher pressure run, the exit pressure had to be increased in GFSSP by 6.70% in order for the inlet pressure and mass flow rate to be identical to that of the experiment. The predicted heat transfer coefficients and wall temperatures for Run 32 are compared with the measured data in Figures 6 and 7 respectively. The observations are similar to the results of previously discussed Run 5.

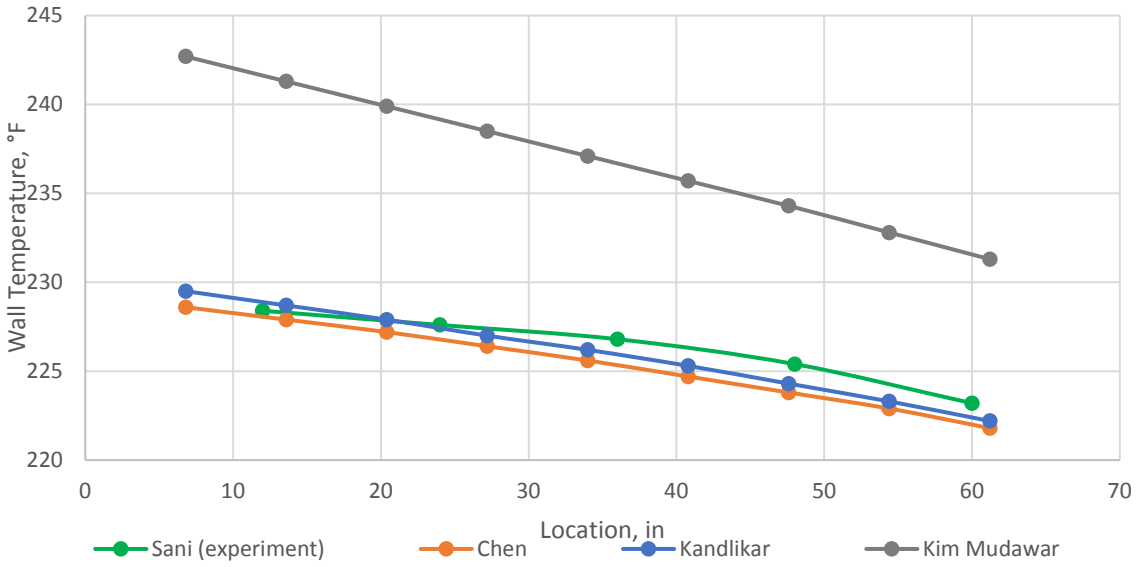

Figure 6. Predicted wall temperatures from correlations compared to experimental wall temperature for Run 5.

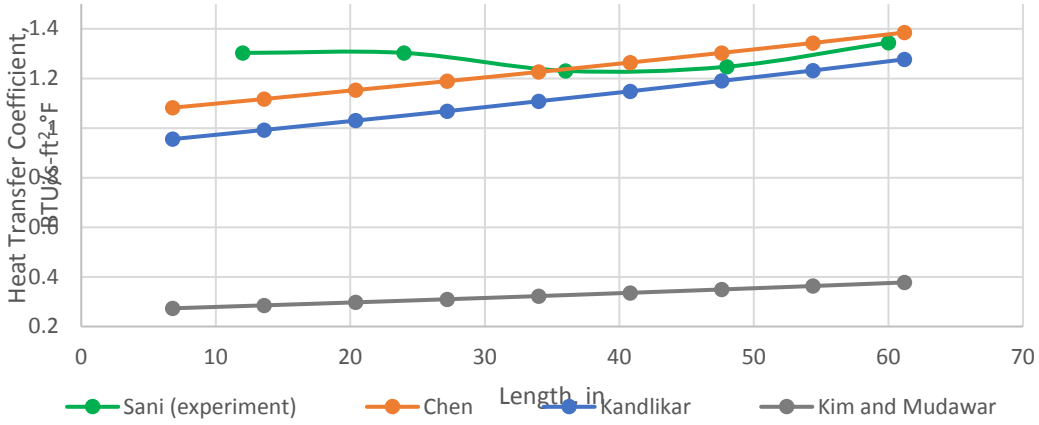

Figure 7. Predicted heat transfer coefficients for Run 32.

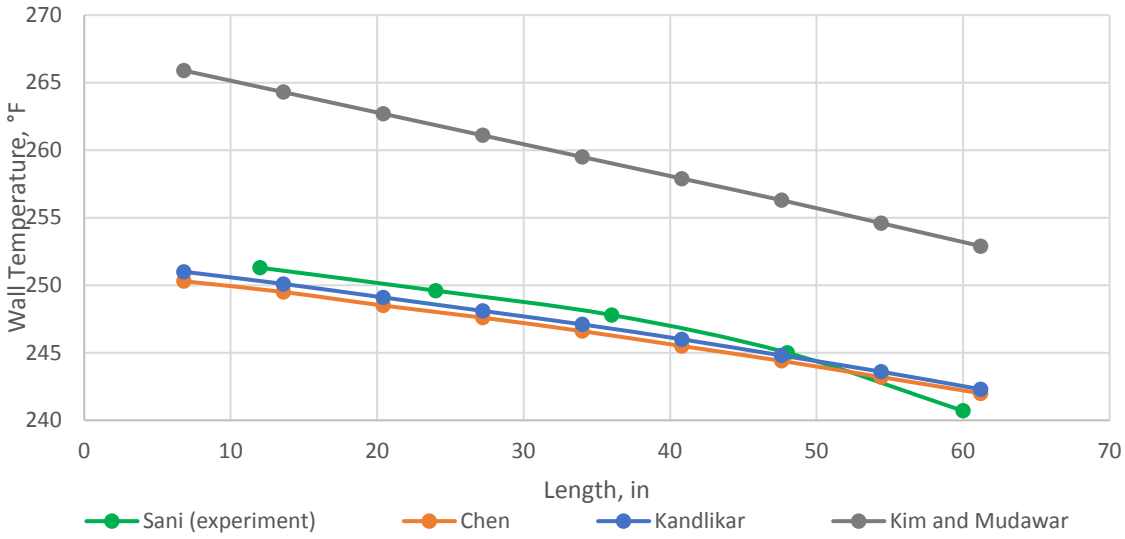

Figure 8. Comparison of predicted wall temperatures versus experimental data for Run 32

5.2 Hendricks et al. Experiment Model

The first Hendricks et al. case tested was Run 18-2. The specification of this test run is given in Table 2. For all of the hydrogen models created, it was observed that to get the inlet pressure and mass flow rates to match the experiment, the outlet pressure had to be set noticeably higher. In this run, the outlet pressure was set 19.1% higher than the experimental value. Figure 9 shows how the model has a much smaller pressure drop throughout the test section compared to the experiment. Nevertheless, the model still provides a close approximation to the experimental fluid temperature data, with a maximum deviation of approximately 0.3% (Figure 10).

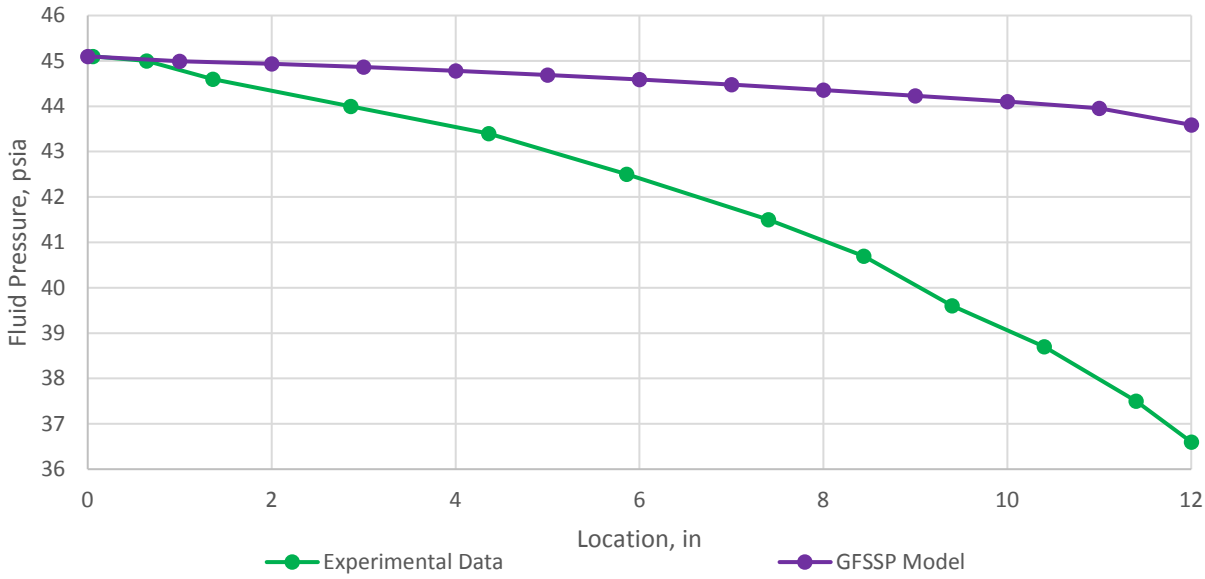

Figure 9. Comparison of experimental and model pressures throughout test section for Hendricks et al. Run 18-2.

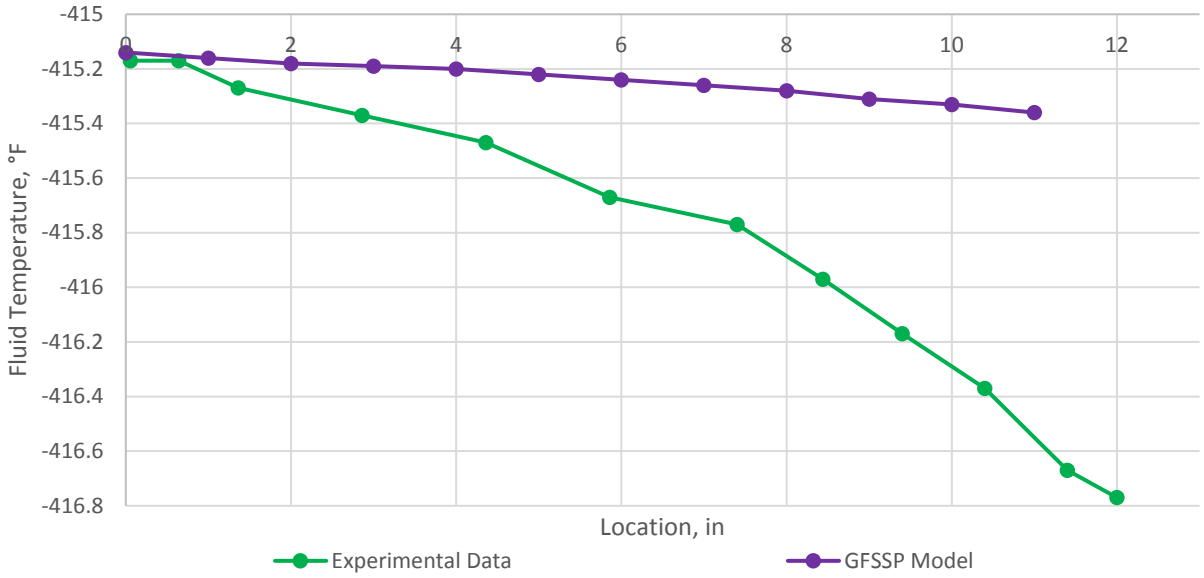

Figure 10. Measured fluid temperatures compared to predicted fluid temperatures for Hendricks et al. Run 18-2.

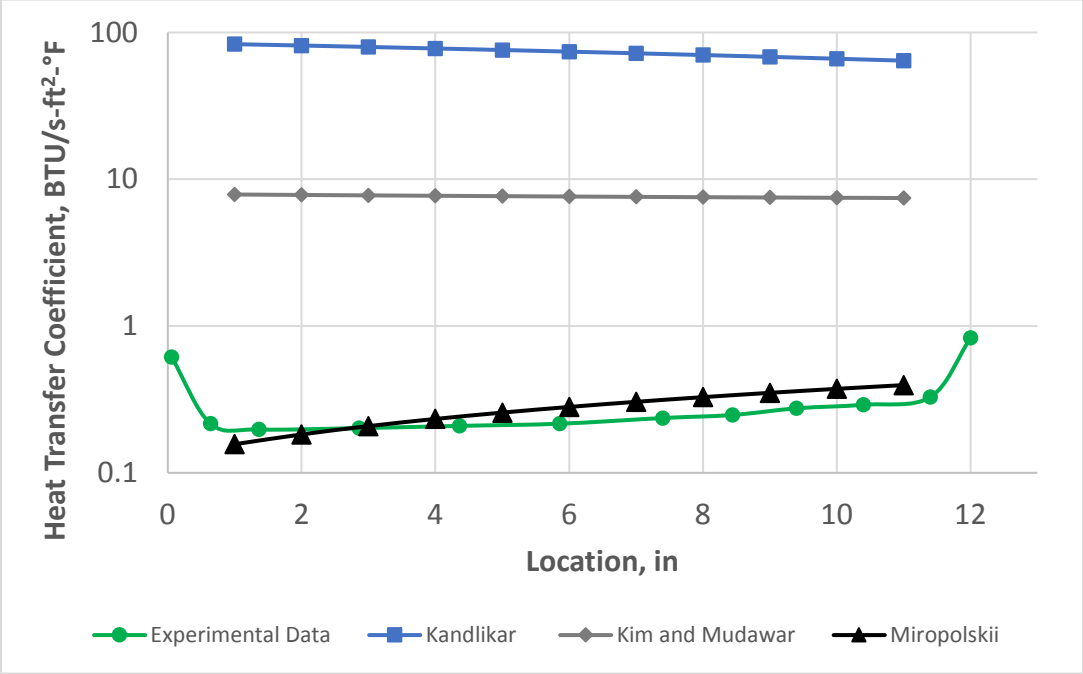

Figure 11. Comparison between correlations' predicted heat transfer coefficients and experimental data for Run 18-2. Note the logarithmic scale.

The computed and measured heat transfer coefficients are shown in Fig. 11. Miropolski's film boiling correlations compare well with the measured data. The large discrepancies between the experimental data and the correlations of Kandlikar and Kim and Mudawar suggest that those correlations are appropriate for nuclear boiling regime whereas Hendrick's experiments were conducted in the film boiling regime.

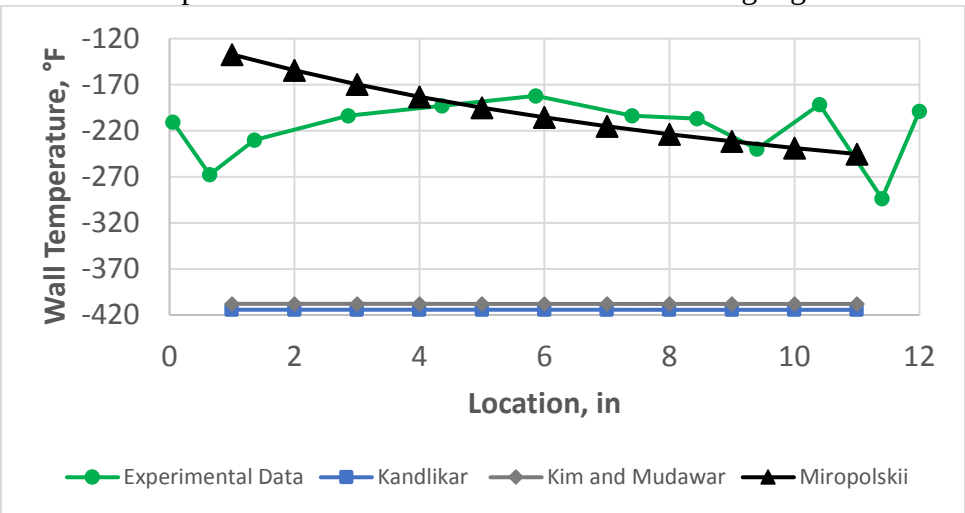

Figure 12. Comparison of experimental and predicted wall temperatures for Run 18-2.

The comparison of experimental and predicted wall temperature with different correlations for Run 18-2 is shown in Fig. 12. As for the heat transfer coefficient, the predicted wall temperatures by Miropolski's film boiling correlation are much closure to the measured wall temperatures, although there are significant discrepancies between the measured and predicted temperatures near the inlet and outlet. The correlations of Kandlikar and Kim and Mudawar predict much lower wall temperatures because of their predicted high heat transfer coefficients of the nuclear boiling regime.

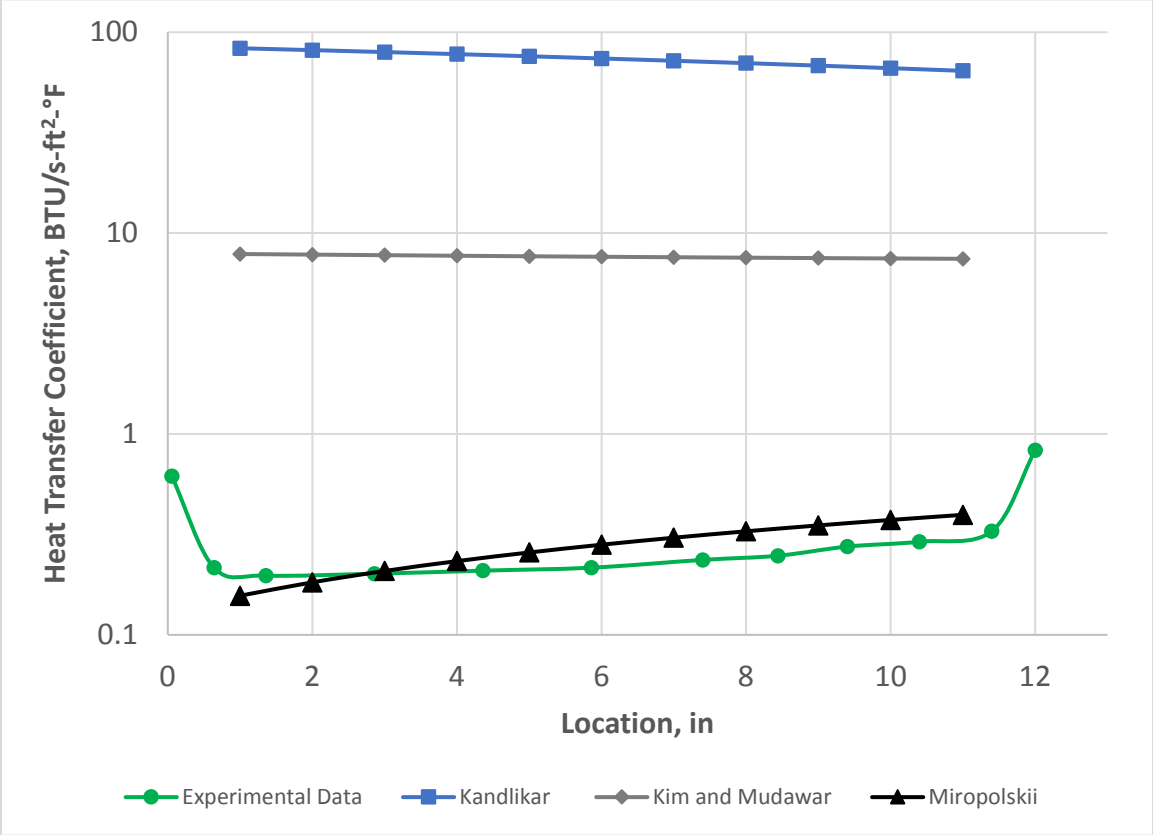

Figure 13. Comparison between correlations' predicted heat transfer coefficients and experimental data for Run 20-5. Note logarithmic scale.

Run 20-5 operated with a higher heat flux, and higher pressure (Table 2). To match the necessary operating conditions, the outlet pressure had to be increased to 36.8% of the experimental value. Fig. 13 shows the comparison of predicted and measured heat transfer coefficients and Fig. 14 shows the comparison of predicted and measured wall temperatures for Run 20-5. The observations are very similar to that of Run 18-2.

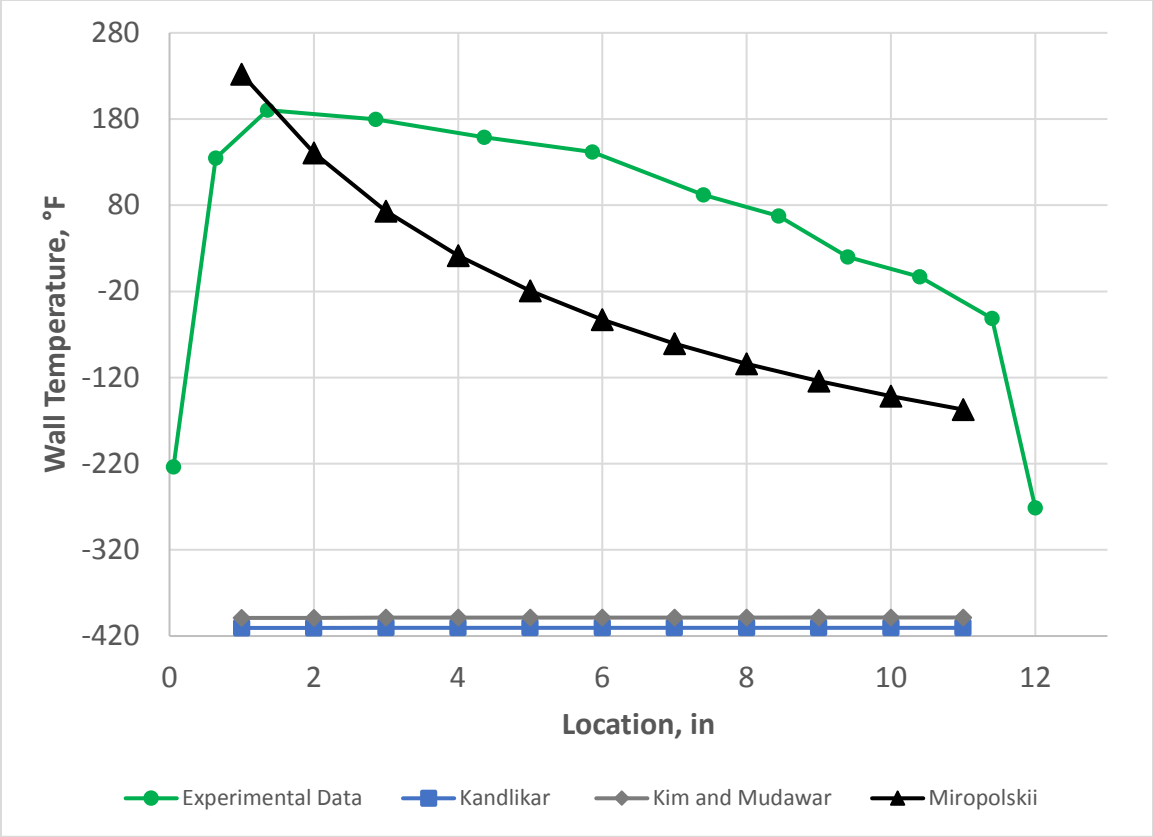

Figure 14. Comparison of experimental and predicted wall temperatures for Run 20-5.

6. Conclusions

A numerical model of boiling in a heated tube has been developed using GFSSP, a general purpose flow network code. Two-phase flow was modeled assuming the flow to be homogeneous. The energy conservation equation for solid wall was solved with the prescribed heat flux, in conjunction with the mass, momentum and energy equations for the fluid. The numerical models were developed for both water and hydrogen and numerical results were compared with test data. Four boiling correlations were used in the model. Three boiling correlations (Chen, Kandlikar, Kim and Mudawar) are appropriate for the nucleate boiling regime. The other boiling correlation (Miropolski) is applicable in the film boiling regime. The results for the modeling of the inner wall temperature and heat transfer coefficient for the boiling of water in a vertical tube demonstrate that the nucleate boiling correlations used in this paper are reasonably accurate. The maximum discrepancy in wall temperatures are within 15%. On the other hand, the experiments with hydrogen were conducted in the film boiling regime; therefore the numerical model with Miropolski's film correlation predicted heat transfer coefficient and wall temperatures more accurately than the nucleate boiling correlations. However, the discrepancies between the measurements and predictions for liquid hydrogen are significantly larger than the

observed discrepancies in experiments with water. It is also observed that the solid wall can be represented by a single node. Discretization of the wall with multiple nodes did not increase the accuracy of predicted wall temperature and heat transfer coefficient.

7. References

[1] S. Kim and I. Mudawar, "Review of databases and predictive methods for heat transfer in condensing and boiling mini/micro-channel flows," International Journal of Heat and Mass Transfer, vol. 77, pp. 627-652, 2014.

[2] S. Kim and I. Mudawar, "Universal approach to predicting two-phase frictional pressure drop for mini/micro-channel saturated flow boiling," International Journal of Heat and Mass Transfer, vol. 58, pp. 718-734, 2013.

[3] M. Shah, "Unified correlation for heat transfer during boiling in plain mini/micro and conventional channels," International Journal of Refrigiration, vol. 74, pp. 606-626, 2017.

[4] M. Shah, "Comprehensive Correlation for Dispered Flow Film Boiling Heat Transfer in Mini/Micro Tubes," International Journal of Refrigeration, vol. 78, pp. 32-46, 2017.

[5] J. Hartwig, S. Darr and A. Asencio, "Assessment of existing two phase heat transfer coefficient and critical heat flux correlations for cryogenic flow boiling in pipe quenching experiments," *International Journal of Heat and Mass Transfer*, vol. 93, pp. 441-463, 2016.

[6] Mercado, M., Wong, N., and Hartwig, J.W. “Assessment of Two-Phase Heat Transfer Coefficient and Critical Heat Flux Correlations for Cryogenic Flow Boiling in Pipe Heating Experiments” *International Journal of Heat and Mass Transfer* 133, 295 – 315. 2019.

[7] Darr, S.R., Hartwig, J.W., Dong, J., Wang, H., Majumdar, A.K., and LeClair, A.C., and Chung, J.N. “Two-Phase Pipe Chilldown Correlations for Liquid Nitrogen and Liquid Hydrogen” *ASME Journal of Heat and Mass Transfer* 141 (4), 042901. 2019.

[8] LeClair, A., Hartwig, J.W., Hauser, D.M., Diaz-Hyland, P.G., and Going, T.R. “Modeling Cryogenic Chilldown of a Transfer Line with GFSSP” *AIAA-2018-4756, 54th Joint Propulsion Conference* Cincinnati, OH, July 9 – 11, 2018.

[9] Sakowski, B., Hauser, D., Hartwig, J.W., and Kassemi, M. “Validation of Heat Transfer Correlations in Line Chilldown Tests of Cryogenic Fluid in SINDA/FLUINT” *AIAA-2018-4884, 54th Joint Propulsion Conference* Cincinnati, OH, July 9 – 11, 2018.

[10] Graham B. Wallis, “One dimensional Two-Phase Flow” , Mcgraw-Hill, 1969.

[11] Cross, M. F., Majumdar, A. K., Bennett Jr., J. C., and Malla, R. B., “Modeling of Chill Down in Cryogenic Transfer Lines,” *Journal of Spacecraft and Rockets*, Vol. 39, No. 2, 2002, pp. 284–289.

[12] Majumdar, A.; and Ravindran, S.S.: “Numerical Modeling of Conjugate Heat Transfer in Fluid Network,” *J. Prop. Power*, Vol. 27, No. 3, pp. 620–630, 2011.

[13] Majumdar, A. K., LeClair, A. C., Moore, R., and Schallhorn, P. A., “Generalized Fluid System Simulation Program, Version 6.0,” NASA/TP-2016-218218, March 2016.

[14] Sani, R. L. R., “Downflow boiling and nonboiling heat transfer in a uniformly heated tube,” Master’s Thesis, University of California, Berkeley, Report No. UCRL 9023, 1960.

[15] Hendricks, R. C., Graham, R.W., Hsu, Y. Y., and Friedman, R., "Experimental Heat Transfer and Pressure Drop of Liquid Hydrogen Flowing Through a Heated Tube," NASA TN D-765, May 1961.
[16] Chen, J. C., "A Correlation For Boiling Heat Transfer To Saturated Fluids In Convective Flow," *I&EC Process Design and Development*, vol. 5, Jul. 1966, pp. 322–329.
[17] Kandlikar, S. G., "A General Correlation for Saturated Two-Phase Flow Boiling Heat Transfer Inside Horizontal and Vertical Tubes," *Journal of Heat Transfer*, vol. 112, Feb. 1990, pp. 219–228.
[18] Kim, S. M., and Mudawar, I., "Universal approach to predicting saturated flow boiling heat transfer in mini/micro-channels – Part II. Two-phase heat transfer coefficient," *International Journal of Heat and Mass Transfer*, vol. 64, 2013, pp. 1239–1256.
[19] Miropolski, Z. L., "Heat Transfer in Film Boiling of a Steam-Water Mixture in Steam Generating Tubes," *Teploenergetika*, Vol. 10, No. 5, 1963, pp. 49–52.
[20] Friedel, L., "Improved Friction Pressure Drop Correlation for Horizontal and Vertical Two-phase Pipe Flow," *European Two-Phase Flow Group Meeting*, 1979.
[21] Collier, J.G and Thome, J.R., "Convective Boiling and Condensation," 3rd Edition, Oxford Science Publications, 1996.